ACS APPLIED MATERIALS & INTERFACES

Research Article

www.acsami.org

Interfacing a Tetraphenylethene Derivative and a Smart Hydrogel for Temperature-Dependent Photoluminescence with Sensitive Thermoresponse

Yingnan Jiang,[†,‡,⊥] Xudong Yang,[†,⊥] Cheng Ma,[†,§] Chuanxi Wang,[†] Yang Chen,[†] Fengxia Dong,[†] Bai Yang,[†] Kui Yu,*[,∥] and Quan Lin*[,†]

[†]State Key Laboratory of Supramolecular Structure and Materials, College of Chemistry, Jilin University, Changchun, 130012, P. R. China

[‡]Lab of Polymer Composites Engineering, Changchun Institute of Applied Chemistry, Chinese Academy of Sciences, Changchun, 130022, P. R. China

[§]Institute of Atomic and Molecular Physics, Sichuan University, Chengdu, 610065, P. R. China

[∥]Emerging Technologies Division, National Research Council of Canada, Ottawa, Ontario, K1A 0R6, Canada

Supporting Information

ABSTRACT: We report, for the first time, the design and synthesis of thermoresponsive (TR) photoluminescent (PL) hydrogel nanoparticles, with a core consisting of poly[styrene-*co*-(*N*-isopropylacrylamide)] (PS-*co*-PNIPAM) and a PNIPAM-*co*-PAA shell. PAA represents polyacrylic acid which interacts with our emitting molecule 1,2-bis[4-(2-triethylammonioethoxy)phenyl]-1,2-diphenylethene dibromide (d-TPE). The electrostatic interaction between each water-soluble d-TPE molecule and two AA repeat units activates these d-TPE molecules to exhibit strong PL. Our d-TPE doped PS-*co*-PNIPAM/PNIPAM-*co*-PAA particles in water display remarkable TR PL: the emission intensity decreased in the course of heating from 2 to 80 °C and recovered during cooling from 80 to 2 °C. Such linear, reversible, and sensitive TR PL is achieved by the use of both PAA and PNIPAM as the shell polymeric chain and by careful optimization of the d-TPE to AA feed molar ratio. Thus, the emission of the d-TPE molecule is affected sensitively by temperature. In addition to such an exceptionally temperature-dependent PL, the presence of CrO_4^{2-} resulted in the decrease of the emission intensity, which was also temperature-dependent. The present study provides a unified conceptual methodology to engineer functional water-dispersible hydrogel nanoparticles that are stimuli-responsive with the potential to advance various PL-based applications.

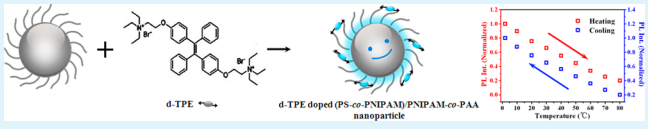

KEYWORDS: *photoluminescent hydrogel nanoparticles, reversible and linear thermoresponses, temperature-dependent photoluminescence, TPE derivatives, CrO_4^{2-} sensing*

INTRODUCTION

Photoluminescent (PL) and water-dispersible hydrogel nanoparticles with sensitive and reversible responses to external stimuli have significant potential in various applications such as thermosensors,[1,2] bioprobes,[3−5] drug delivery vehicles,[6−8] and chemosensors.[9−13] Among a large variety of photoemission candidates, tetraphenylethene (TPE) and its derivatives have attracted much attention because of their low PL in solution and substantially enhanced PL resulting from molecular immobilization.[4,14−21] Such an exceptional event, also documented as aggregation-induced emission (AIE), has been related to the restricted intramolecular rotation (RIR) of the four phenyl groups. To maintain a desirable temperature dependence of the ring-flipping processes, the importance of having two of the four phenyl rings unsubstituted has been highlighted.[17] To implement the RIR process of the AIE molecules for immobilization-induced emission (IIE),[3−5,12−29] several approaches have been developed, which include copolymerization with *N*-isopropylacrylamide (NIPAM),[21−23] encapsulation in polymers,[24,25] confinement within rigid porous metal−organic frameworks,[17,18] aggregation induced by formation of nanostructures,[26−28] and solidification at a temperature lower than the freezing point of solvent.[16,29] Favorably, the cytotoxicity of the TPE derivatives was argued to be lower than that of colloidal PL inorganic quantum dots, such as CdTe.[4,14−16,30] The AIE luminogens have been reported to exhibit enhanced PL at low temperatures due to the RIR process; however, their thermoresponsive (TR) PL has not been very sensitive, reversible, or controllable.[4,14−16,21,29]

Among the PL stimuli-responsive hydrogels, poly(*N*-isopropylacrylamide) (PNIPAM) based fluorescent hydrogels have attracted much attention.[1,6,9,21−23,30] PNIPAM has been well acknowledged as a TR polymer, displaying a lower critical solution temperature (LCST) of 32 °C in water with a reversible coil-to-globule transition. Usually, the PNIPAM-based fluorescent hydro-

Received: August 27, 2013
Accepted: March 4, 2014
Published: March 4, 2014

dx.doi.org/10.1021/am501106x | ACS Appl. Mater. Interfaces 2014, 6, 4650−4657

gels, reported from other research groups, exhibit an on−off feature during the temperature change around the PNIPAM LCST.[1,6,9,21−23,30] An on−off PL feature imposes limits on potential applications, compared to a continuously TR PL system.

Recently, we designed and synthesized Eu-doped smart hydrogel nanoparticles that exhibit sensitive and reversible TR PL in the temperature range of 10−50 °C.[31] The hydrogel nanoparticles consisted of a core−shell structure, with the core of poly[styrene-*co*-(*N*-isopropylacrylamide)] (PS-*co*-PNIPAM) and the shell of PNIPAM. The photoluminescent entity was Eu(III) phthalate which was made from the reaction of $EuCl_3$ and phthalic acid in water. This water-soluble europium organic complex exhibits two emission peaks at ∼590 and ∼615 nm. Via the interaction with the amide group of PNIPAM chain, the Eu(III) complex was coordinated in the PNIPAM shell. The resulting Eu(III)-doped hydrogel nanoparticles exhibited appreciably superior TR PL compared to those of previously-reported PNIPAM hydrogels.[1,21,30]

Here, we report the design and synthesis of our innovative hydrogel nanoparticles exhibiting a single emission peak at ∼468 nm with significantly improved TR PL over a much broader temperature range of 2−80 °C. To the best of our knowledge, there has been no successful fabrication of smart hydrogel nanoparticles that exhibit temperature-dependent PL with a continuously varying emission intensity over the temperature range of 2−80 °C. These novel hydrogel nanoparticles consist of a core−shell structure, with the core of poly[styrene-*co*-(*N*-isopropylacrylamide)] (PS-*co*-PNIPAM) and the shell of PNIPAM-*co*-PAA. Polyacrylic acid (PAA) interacts with our selected emitting molecule 1,2-bis[4-(2-triethylammonio-ethoxy)phenyl]-1,2-diphenylethene dibromide.[14] This water-soluble TPE derivative, symbolized as d-TPE, has two positively charged sites per molecule. Thus, one d-TPE molecule could be tightly immobilized via the interaction between its two positively-charged sites and two negatively-charged carboxyl groups of two AA repeat units. Such immobilization instigated strong PL of the d-TPE molecule. At the same time, TR PNIPAM together with PAA facilitated the d-TPE doped PS-*co*-PNIPAM/PNIPAM-*co*-PAA nanoparticles in water to exhibit sensitive temperature-dependent PL in the temperature change of 2−80 °C. The observed TR PL is linear and reversible. Regarding the shell composition and the emission molecule, the novelty of the present system is obvious, compared to our previous system.[31] Furthermore, with a proper d-TPE to AA feed molar ratio, the resulting photoluminescent nanoparticles exhibit good colloidal stability in a wide range of pH and ionic strength. In the presence of CrO_4^{2-}, these smart hydrogels displayed reduced emission in intensity. The expected electron transfer from the d-TPE molecule to CrO_4^{2-} effectively weakens the emission intensity of the d-TPE doped hydrogel nanoparticles effectively. Our unprecedented TR PL hydrogels should be able to enrich the potential applications of the TPE-type molecules, since they function over a broad temperature range.[4,14−21,24] Furthermore, the present design and synthesis of the d-TPE-doped PS-*co*-PNIPAM/PNIPAM-*co*-PAA hydrogel nanoparticles should shed light on a general methodology that leads to functional hydrogels with sensitive responses to external stimuli.[15,16]

EXPERIMENTAL SECTION

Chemicals and Materials. *N*-Isopropylacrylamide (NIPAM) was purchased from Acros. Styrene (St) and acrylic acid (AA) were purified by vacuum distillation, and potassium persulfate (KPS) was purified by crystallization from water. Double-distilled water purified by the Millipore Milli-Q system was used in all experiments. The ammonium salt of a TPE derivative 1,2-bis[4-(2-triethylammonioethoxy)phenyl]-1,2-diphenylethene dibromide (d-TPE) was supplied by Prof. Benzhong Tang and Prof. Jingzhi Sun,[14,20] with its ^1H and ^{13}C NMR presented in Figures S1 and S2, respectively.

Preparation of PS-*co*-PNIPAM Core Nanoparticles and PS-*co*-PNIPAM/PNIPAM-*co*-PAA Core−Shell Nanoparticles. The detailed procedure for the synthesis of the core and the core−shell nanoparticle can be found elsewhere but with modification.[31−33] The PS-*co*-PNIPAM nanoparticles were synthesized by emulsifier/surfactant-free emulsion copolymerization.[31,32] NIPAM (∼0.5 g = 4.4 mmol) was dissolved in deionized water (∼15 mL) in a 250 mL three-necked round-bottom flask equipped with a stirrer, a condenser, and a nitrogen inlet. Afterward, styrene (∼5.0 mL = 50.0 mmol) and deionized water (∼175 mL) were added into the reaction flask. Under N_2 atmosphere, the mixture was stirred at room temperature for ∼30 min to remove oxygen, and the temperature was increased to 70 °C. An initiator solution of ∼0.1 g of potassium persulfate (KPS) in ∼10 mL of deionized water was swiftly injected into the reaction mixture after 10 min. The reaction was allowed to proceed for ∼8 h under N_2 with stirring. The prepared PS-*co*-PNIPAM nanoparticles were purified three times by centrifugation and dispersion in deionized water. The as-prepared PS-*co*-PNIPAM core nanoparticles in water are very stable, as presented in our previous work.[31]

For the nanoparticle shell, monomer acrylic acid (AA) was used because of its nature of negative charge, with AA to NIPAM feed molar ratios in the range of 2−20%. The PNIPAM-*co*-PAA shells were grafted on the purified PS-*co*-PNIPAM nanoparticles by seed emulsion polymerization; no surfactant was used either.[31−33] For a typical synthesis, the purified PS-*co*-PNIPAM nanoparticles were dispersed in deionized water (∼185 mL) in a 250-mL three-necked round-bottom flask. NIPAM (∼4.5 g = 39 mmol) and AA (∼0.112 g = 1.56 mmol) were added to the reaction flask. The reaction molar ratio of AA to NIPAM is ∼4%. Similarly, under N_2 atmosphere, the mixture was stirred at room temperature for ∼30 min to remove oxygen, and the temperature was increased to 70 °C. At 10 min later, an initiator solution of ∼0.1 g of KPS in ∼15 mL of deionized water was swiftly injected into the reaction mixture. The reaction was allowed to proceed for ∼8 h under N_2 with stirring. Again, the resulting PS-*co*-PNIPAM/PNIPAM-*co*-PAA hydrogel nanoparticles were purified three times by centrifugation and dispersion in deionized water. The purified core−shell nanoparticles were dispersed in ∼200 mL of deionized water, as a stock dispersion.

Preparation of d-TPE Doped PS-*co*-PNIPAM/PNIPAM-*co*-PAA Hydrogel Nanoparticles. Under N_2, the TPE derivative with two positively charged sites per molecule was introduced to the core−shell nanoparticles in water at 32 °C, with d-TPE to AA feed molar ratios of 5×10^{-4} to 1×10^{-2}. For a typical synthesis, water-soluble TPE derivative d-TPE (∼0.1875 mg = 0.26 μmol) was mixed with the PS-*co*-PNIPAM/PNIPAM-*co*-PAA nanoparticles (∼10 mL stock dispersion) in a 100 mL round-bottomed flask. The molar ratio of d-TPE to AA is $\sim 3 \times 10^{-3}$. The reaction mixture was stirred at 32 °C under N_2 for 3 h. Finally, the d-TPE doped PS-*co*-PNIPAM/PNIPAM-*co*-PAA nanoparticles were prepared and purified once by centrifugation. The purified d-TPE doped PS-*co*-PNIPAM/PNIPAM-*co*-PAA nanoparticles were dispersed in ∼25 mL water, as a stock dispersion.

Characterization. PL spectra were collected with a Shimadzu RF-5301 PC spectrophotometer with an excitation wavelength of 340 nm. Digital photos were taken upon irradiation with a UV lamp of 365 nm. Dynamic light scattering (DLS) measurement was carried out by a Zetasizer NanoZS (Malvern Instruments). Scanning electron microscope (SEM) images were performed by a JEOL FESEM 6700F electron microscope with primary electron energy of 3 kV. ^1H NMR was obtained on a Varian NMR spectrometer (300 MHz). ^{13}C NMR (500 MHz) was executed on the AVANCEIII500 (Bruker).

RESULTS AND DISCUSSION

In the present study, three d-TPE doped PS-*co*-PNIPAM/PNIPAM-*co*-PAA core−shell nanoparticle samples (AA to NIPAM feed molar ratios, d-TPE to AA feed molar ratios) are

Scheme 1. Schematic Drawing of the Approach To Synthesize the d-TPE Doped PS-*co*-PNIPAM/PNIPAM-*co*-PAA Hydrogel Nanoparticles Exhibiting Sensitive, Linear, and Reversible TR PL in the Temperature Range of 2−80 °C[a]

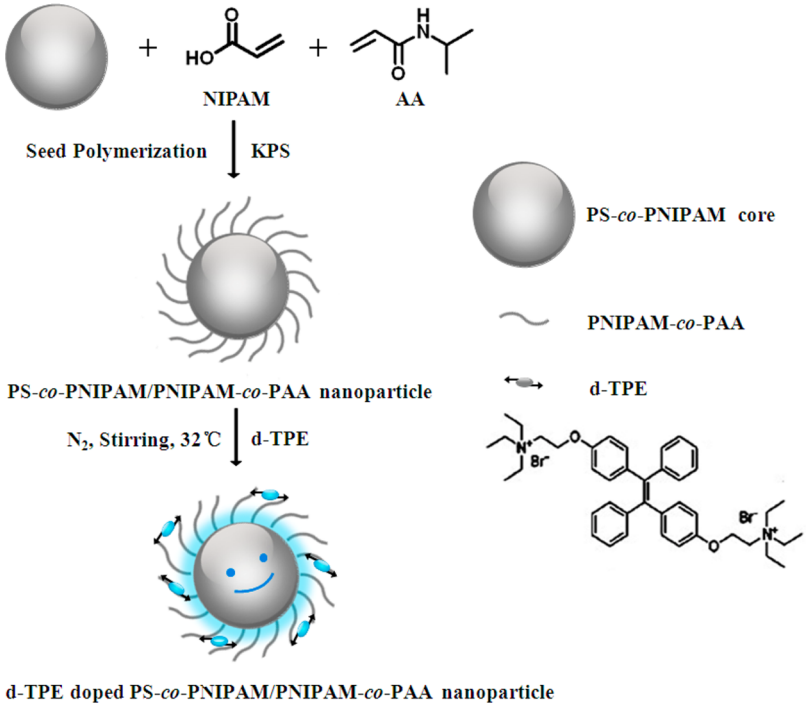

[a]See Figure S3 for the significant increase in emission after d-TPE is incorporated into the hydrogel nanoparticles.

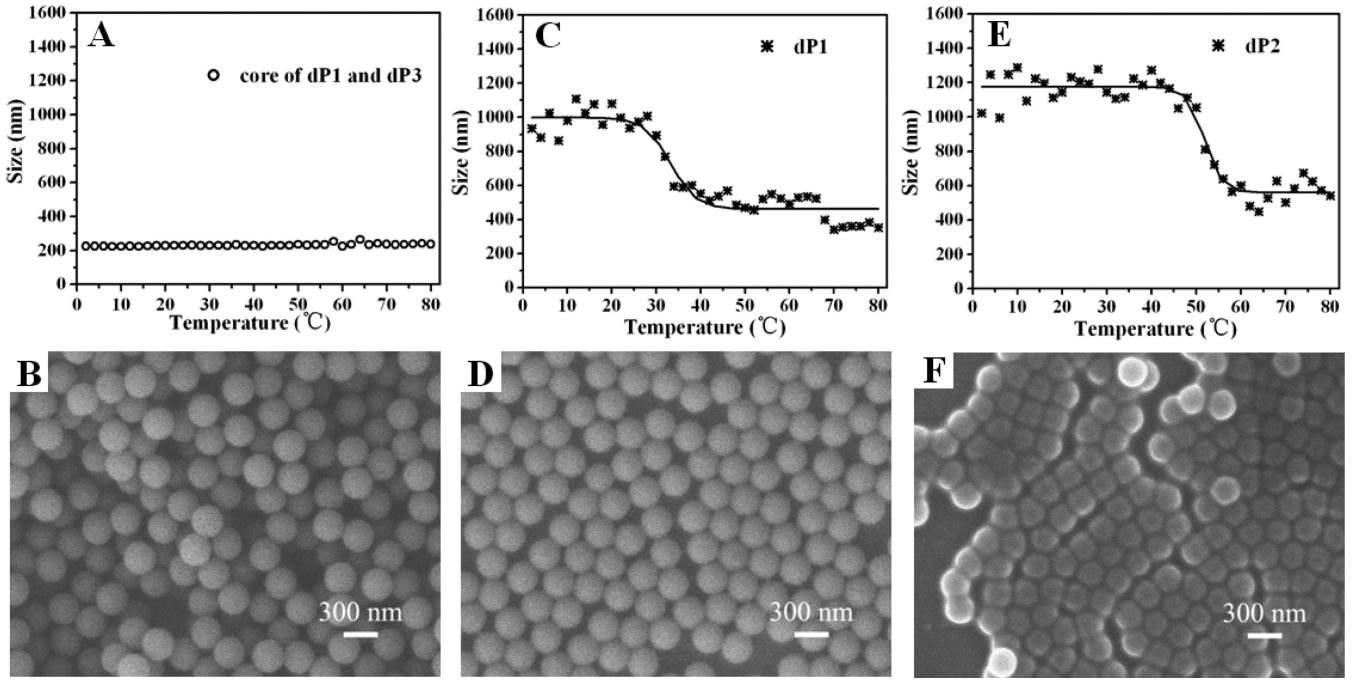

Figure 1. DLS measurements (top) and SEM images (bottom) of the PS-*co*-PNIPAM core (A, B) and the d-TPE doped hydrogel nanoparticles (C−F). For the core of dP1 and dP3, the SEM diameter is ∼268 nm (B). One SEM image of the dP2 core (∼226 nm) is shown in Figure S4. For dP1 and dP3, the lower critical solution temperature (LCST) is estimated to be ∼34 °C (C) with the SEM diameter of ∼281 nm (D). For dP2, the LCST is estimated to be ∼52 °C (E), with the SEM diameter of ∼250 nm (F).

presented: dP1 (4%, 3×10^{-3}), dP2 (16%, 3×10^{-3}), and dP3 (4%, 8×10^{-4}). See Table S1. Scheme 1 illustrates our synthetic route to the d-TPE doped PS-*co*-PNIPAM/PNIPAM-*co*-PAA core−shell hydrogel nanoparticles which exhibit temperature-dependent PL in the temperature range of 2−80 °C.

After the water-soluble d-TPE molecule, which weakly emits PL, was incorporated into the shell of the PS-*co*-PNIPAM/PNIPAM-*co*-PAA hydrogel nanoparticles via the electrostatic interaction, enhanced emission centered at ∼468 nm was immediately observed. The top part of Figure S3 presents two

dx.doi.org/10.1021/am501106x | *ACS Appl. Mater. Interfaces* 2014, 6, 4650−4657

emission spectra acquired at 2 °C, with the gray curve from one d-TPE solution in water and the blue curve from a dP1 aqueous dispersion. Also, digital photos of the two samples under the irradiation from a 365 nm UV lamp are provided. The two dispersions had a similar amount of the emitting molecule, d-TPE. Undoubtedly, the dP1 dispersion is much brighter than the d-TPE solution. Obviously, the electrostatic interaction between the d-TPE molecules and the PNIPAM-*co*-PAA chains substantially hindered the intramolecular motion of the d-TPE molecules. Accordingly, immobilization-induced emission (IIE) was obtained. When a small amount of the d-TPE molecules are doped, the resulting hydrogel nanoparticles can exhibit bright emission. The bottom part of Figure S3 shows the corresponding PL excitation and emission spectra.

Dynamic light scattering (DLS, in the above panel of Figure 1) was used to examine particle sizes at different temperatures. During the temperature increase in the range of 2−80 °C, the core nanoparticles exhibited little change in size while the d-TPE doped core−shell hydrogel nanoparticles exhibited a noticeable decrease in size. Fascinatingly, the colloidal and thermal stability of the PS-*co*-PNIPAM core and the d-TPE doped PS-*co*-PNIPAM/PNIPAM-*co*-PAA hydrogel nanoparticles in water is high. With an increase of the AA to PNIPAM feed molar ratio from 4% (dP1, dP3) to 16% (dP2), the lower critical solution temperature (LCST) seemed to increase from ∼34 to ∼52 °C.[6,33]

Corresponding SEM images are displayed in the lower portion of Figure 1, demonstrating narrow size distribution. The SEM size information of dP1, dP2, and dP3 is summarized in Table S1. The core of dP1 and dP3 is ∼268 nm (Figure 1B), and the core of dP2 is ∼226 nm (Figure S4, top). The dP1 and dP2 sizes are estimated to be ∼281 nm (Figure 1D) and ∼250 nm (Figure 1F), respectively. The detailed DLS analysis of the as-prepared nanoparticles at room temperature is also shown in Figure S5. Note that the hydrodynamic diameter of dP2 (Figure1E) is larger than that of dP1 (Figure 1C), and the significant change in size around the LCST is worthy of notice.[33]

Figure 2A shows six digital photos. The left-most photo is one d-TPE solution in water at 2 °C, and the remaining five from left to right are dP1 dispersions (Figure 1C) in water at 2, 20, 40, 60, and 80 °C. The six vials were under UV illumination by a lamp of 365 nm. Figure 2B illustrates eight emission spectra obtained from an aqueous d-TPE solution when the temperature increased by 10 steps from 10 °C to 80 °C. Figure 2C presents 40 emission spectra collected from dP1 in water during the increase of temperature from 2 to 80 °C, with each step of 2 °C. It took ∼2 min for the 2 °C increase per step and less than 2 h to acquire the 40 spectra. Amazingly, the emission intensity decreased steadily and almost linearly, as shown in Figure 2D (open blue circular symbols, left y axis). The two dispersions shown in Figure 2B and Figure 2C have an identical concentration of the emitter, the d-TPE molecule. It is clear that the d-TPE molecule, by itself, emits weakly, and its TR PL is summarized in Figure 2D (open dark triangular symbols, right y axis). Moreover, the PL of the hydrogel nanoparticles (derived from the IIE process) decreased gradually from 2 to 80 °C. While the TR PL of the particle doped with d-TPE is linear, the size of the PS-*co*-PNIPAM@PNIPAM-*co*-PAA particles changes sharply around LCST (Figure 1C). Thus, the TR PL seems to be affected little by the size of the particle but mainly by the temperature. It has been acknowledged that higher temperature provides more energy to activate intramolecular rotation and vibration of d-TPE, and such activation is accompanied by a strong reduction of the PL intensity.[15,16,29] In our system, the

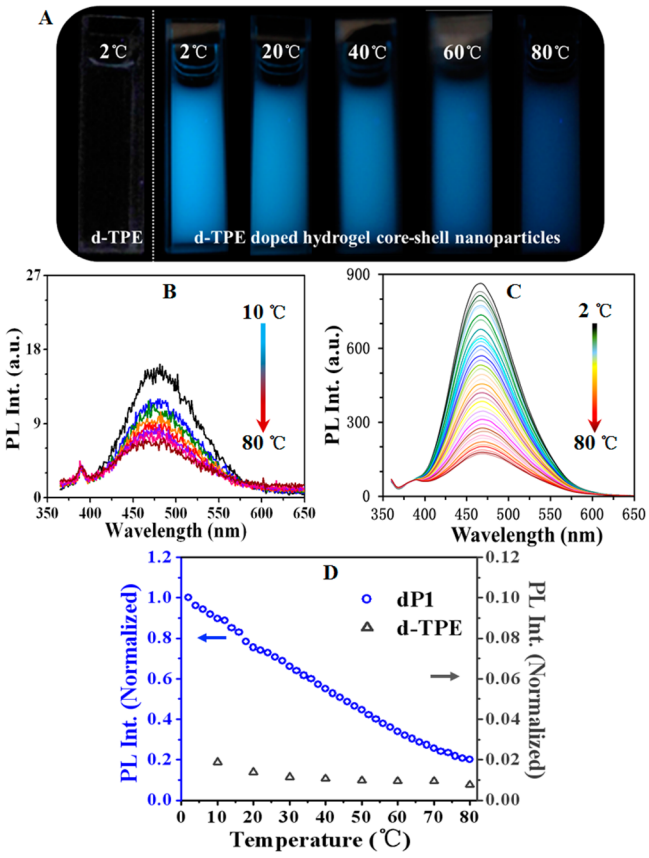

Figure 2. (A) Digital photos of one d-TPE aqueous solution (left-most) and other right five dP1 aqueous dispersions under the irradiation with a UV lamp of 365 nm. (B) Eight PL spectra (with λ_{ex} of 345 nm) of the d-TPE aqueous solution acquired in the course of temperature increase from 10 to 80 °C with a step 10 °C. (C) 40 PL spectra (with λ_{ex} of 345 nm) of the dP1 aqueous dispersions collected in the course of temperature increase from 2 to 80 °C with a step of 2 °C. (D) Comparison of the TR PL of the d-TPE solution (B, right axis) and the dP1 dispersion (C, left axis).

combination of PAA and PNIPAM chains may provide a fortuitous temperature dependent inhibition of the intramolecular rotation and vibration of d-TPE, causing the continuous variation of PL emission intensity with temperature, and the effect of the shrinkage of the PNIPAM chain near the LCST on the PL is small.

Figure 3 demonstrates the PL intensity change of the three samples dP1, dP2, and dP3 in the course of temperature increase from 2 to 80 °C. The PL intensity change is almost linear with the temperature. The corresponding PL spectra are displayed in Figure S6.

Intriguingly, the d-TPE doped hydrogel nanoparticles exhibit TR PL which appears to be reversible with temperature. Figure 4A demonstrates that the emission intensity is almost perfectly recovered during one temperature cycle. When the temperature was increased from 2 to 10 °C and then with a step 10−80 °C, the emission intensity of the d-TPE doped hydrogel nanoparticles (dP1) decreased linearly (left *y* axis and nine red squares). Next, when the temperature was decreased back, from 80 to 2 °C, the emission intensity recovered (right *y* axis and nine blue squares). The corresponding emission spectra collected from this dP1 sample in water is shown in Figure S6a. Note that the d-TPE to AA feed molar ratio affects the colloidal stability at temperatures higher than the LCST. Figure 2A and Figure S7 show that when

dx.doi.org/10.1021/am501106x | ACS Appl. Mater. Interfaces 2014, 6, 4650−4657

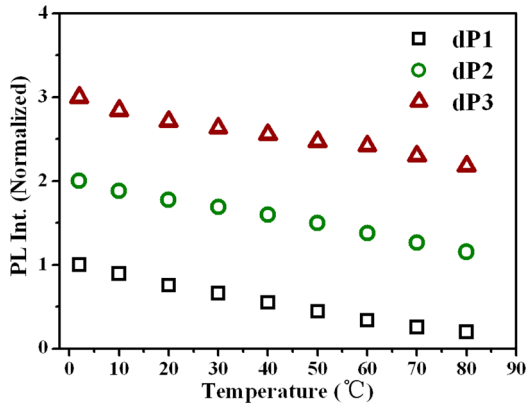

Figure 3. For the three samples, dP1 (4%, 3×10^{-3}), dP2 (16%, 3×10^{-3}), and dP3 (4%, 8×10^{-4}), the change of PL intensity (dP2 offset 1 from dP1, and dP3 offset 1 from dP2) from 2 to 80 °C.

the d-TPE to AA feed molar ratio was 3×10^{-3}, good dispersion was obtained even at 80 °C; however, when the d-TPE to AA feed molar ratio was 1×10^{-2}, a phase transition took place at 40 °C. With a proper d-TPE to AA feed molar ratio, neither the pH (Figure S10) nor the ionic strength (Figure S11) had a significant effect on the TR PL properties.

Evidently, our smart d-TPE doped hydrogel nanoparticles exhibit temperature-dependent PL, which can also be verified by multiple heating and cooling cycles between 20 and 60 °C, as presented in Figure 4B. At 20 °C, the emission intensity is almost constant and higher than that obtained at 60 °C. Each step of the 40 °C heating or cooling took ~30 min, the shortest time that could be achieved by our instrument. Figure S8 presents the corresponding eight emission spectra with four collected at 20 °C and the other four at 60 °C.

It seemed appealing to us to understand, in depth, such temperature-determined PL of the d-TPE doped hydrogel nanoparticles. Accordingly, we designed a similar nanoparticle system consisting of polystyrene-*co*-polyacrylic acid (PS-*co*-PAA) with a 100St-to-5AA feed molar ratio. To dope the PS-*co*-PAA nanoparticles, the d-TPE to AA feed molar ratio was 2.5×10^{-3}, similar to that of the dP1 sample. Figure 4C summarizes the emission intensity obtained, when the temperature was increased from 10 to 70 °C with a step of 10 °C (seven red squares) and then decreased back to 20 °C (five blue squares). Undoubtedly, as demonstrated by this cycle with heating first and then cooling, the difference in emission intensity seems to be larger at a relatively lower temperature such as 20 °C than that at a relatively higher temperature such as 50 °C. Figure S9a presents the corresponding 12 emission spectra, and Figure S9b shows a SEM image of the d-TPE doped PS-*co*-PAA nanoparticles prepared.

Undoubtedly, the TR PL of the d-TPE doped hydrogel nanoparticles is much more sensitive than that of the d-TPE doped PS-*co*-PAA nanoparticles. It is easy to understand that for the two nanoparticle systems, the degree of immobilization of the d-TPE molecule was similar. However, during the course of temperature change, for the former, the extensive motion of the temperature-dependent PNIPAM-*co*-PAA chains assists d-TPE to respond relatively fast (one PL emission intensity at one temperature), compared to the d-TPE molecule on the latter. Such a hypothesis is supported by the fact that for the latter, the difference in emission intensity decreased from 10 to 70 °C after the cycle of heating first and then cooling; the d-TPE molecule responded faster to temperature change at higher temperatures (with more energy provided) than at lower temperatures. It seems reasonable that our PNIPAM-*co*-PAA chains play a major role for our d-TPE doped hydrogel nanoparticles to display the linear and reversible TR PL. Evidently, our PS-*co*-PNIPAM/PNIPAM-*co*-PAA hydrogel nanoparticles bring insights on the design and synthesis of various practical systems to be doped by functional entities for sensitive responses to external stimuli.

Let us turn our attention to chemical sensing. Our TR PL hydrogel nanoparticles are a good candidate system to implement the potential of optical sensing of AIE molecules.[15,16] One example is shown in Figure 5, the detection of chromate anion CrO_4^{2-} in water. Industrial manufacturing processes and environmental erosion produce CrO_4^{2-}, which can enter cells to damage DNA through nonspecific anion channels with facilitated diffusion.[12,13,34−36] Figure 5 illustrates that the presence of Na_2CrO_4 causes a very strong decrease of the PL of our d-TPE doped hydrogel nanoparticles dP1, compared to the five chemicals studied including Na_2SO_4, Na_2CO_3, $NaNO_2$, and $NaHCO_3$. Figure 5A and Figure 5B summarize the emission intensity of the dP1 aqueous dispersions with and without the presence of the five chemicals at 10 and 40 °C, respectively. The concentration of the five salts was 20 mg/L. See Figure S11 for the emission spectra collected with the presence of 20 mg/L Na_2SO_4, Na_2CO_3, $NaNO_2$, and $NaHCO_3$, during the temperature increase from 10 to 50 °C with a step of 10 °C.

Figure 5C summarizes the emission intensity of the dP1 aqueous dispersions with the presence of different amounts of Na_2CrO_4 and at different temperatures. A similar temperature dependent response of the PL of the dP1 sample in water is observed for all studied Na_2CrO_4 concentrations in this temperature range. With the presence of Na_2CrO_4 of 0.5 mg/L (dark yellow open squares), 1 mg/L (dark yellow open

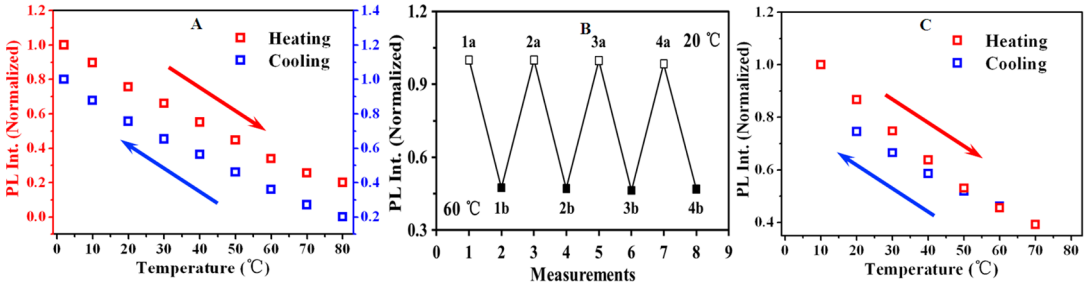

Figure 4. (A) Change of the PL intensity (normalized) of the dP1 aqueous dispersion peaking at ~468 nm during the temperature increase from 2 to 80 °C with eight steps and subsequent decrease back to 2 °C with eight steps. (B) Change of the PL intensity of the dP1 aqueous dispersion during the temperature increase directly from 20 to 60°C and back to 20 °C, of which the corresponding spectra collected shown in Figure S8. (C) Change of the PL intensity (normalized) of the d-TPE doped PS-*co*-PAA nanoparticles in water during the temperature increase from 10 to 70 °C and subsequent decrease from 70 to 20 °C.

dx.doi.org/10.1021/am501106x | *ACS Appl. Mater. Interfaces* 2014, 6, 4650−4657

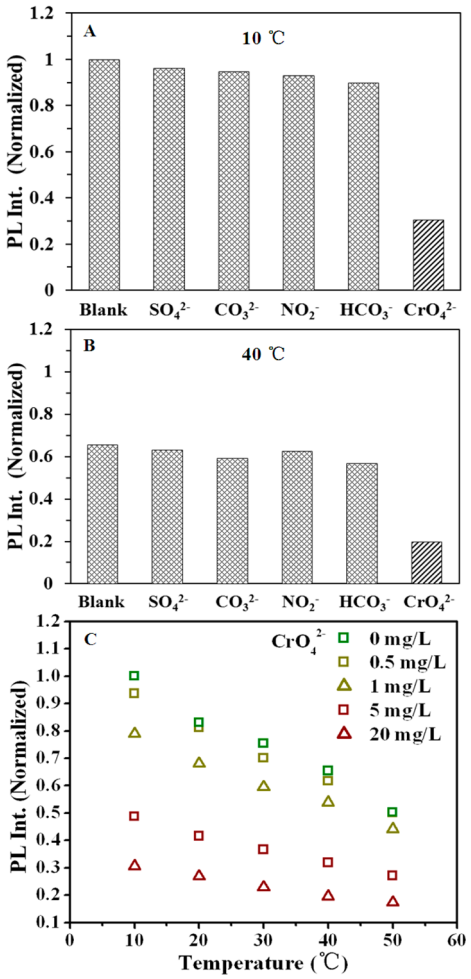

Figure 5. PL intensity (normalized) of our dP1 aqueous dispersions in the presence of the five salts at the same concentration of 20 mg/L at 10 °C (A) and 40 °C (B). (C) PL intensity (normalized) of the dP1 aqueous dispersions during the temperature increase from 10 to 50 °C with a step of 10 °C, in the presence Na_2CrO_4 with different concentrations, as indicated.

triangles), 5 mg/L (wine open squares), or 20 mg/L (wine open triangles), the TR PL of the dP1 sample in water, during the course of the temperature increase from 10 to 50 °C with a step of 10 °C, is very much similar to each other and to that without the presence of Na_2CrO_4 (green open squares, 0 mg/L). See Figure S12 for the corresponding emission spectra acquired with the presence of Na_2CrO_4 at the five concentrations from 0 to 20 mg/L. For a given temperature, the PL emission intensity decreases steadily with increasing CrO_4^{2-} concentration. Interestingly, when the temperature is increased from 10 to 50 °C, the relative change of the emission intensity is almost a constant for the five Na_2CrO_4 concentrations.

$$(I_{10°C} - I_x)/I_{10°C} = \text{constant} \quad (1)$$

where I_x represents the emission intensity obtained at temperature x. Furthermore, the emission intensity is still temperature-dependent, as demonstrated in Figure S12g.

Accordingly, we argue that the decrease of the emission intensity in the presence of CrO_4^{2-} is related to the electron transfer between d-TPE as the electron donor and CrO_4^{2-} as the strong electron acceptor. Such electron transfer weakens the interaction between the d-TPE molecule and the AA repeat units and thus results in decreased emission of the d-TPE molecule. On the basis of the mechanism of the electron transfer, the detection of CrO_4^{2-} could be quantitative in a broad temperature range. The detection sensitivity could probably be related to the amount of the d-TPE molecule: the fewer the d-TPE molecules that are immobilized (to one hydrogel nanoparticle), the lower is the detection limit that could be achieved. This argument is in agreement with our experimental observation on the CrO_4^{2-} detection by d-TPE doped PNIPAM-*co*-PAA polymer brushes.[36] Practically, the detection of a single CrO_4^{2-} anion could become possible when our hydrogel nanoparticle is doped with one d-TPE molecule, if the decrease of the emission intensity of one d-TPE molecule could be sensed. The present study does not address this exciting hypothesis on detection sensitivity any further, but this potential detection sensitivity may have future importance for applications such as industrial waste water monitoring and environmental screening for water protection.

CONCLUSIONS

We designed and synthesized TR PL hydrogel nanoparticles, the emission intensity of which is temperature-dependent in the range of 2−80 °C. Such sensitive TR PL is attributed to the unique structures of both the d-TPE molecule which is a water-soluble ammonium salt and the core−shell hydrogel nanoparticle which is water-dispersible with its colloidal stability provided by its PNIPAM-*co*-PAA shell. The d-TPE molecule has two positively charged sites per molecule, and the core−shell nanoparticle has negatively charged carboxyl groups on its shell. Accordingly, each d-TPE molecule could be tightly immobilized via its two positively charged sites to two carboxyl groups of two AA repeat units, causing a strong immobilization-induced emission. In the course of heating and cooling cycles, both PAA and TR PNIPAM assisted the immobilized d-TPE molecule to respond quickly, leading to reversible and linear temperature-dependent PL. The feed d-TPE to AA molar ratio was optimized for the resulting PL hydrogel particles to form stable dispersions over the broad temperature range of 2−80 °C. In the presence of CrO_4^{2-}, our d-TPE doped hydrogel nanoparticles maintained their temperature-dependent PL but with decreased emission intensity. The electron transfer between d-TPE and CrO_4^{2-} appeared to reduce the PL efficiency of the d-TPE doped hydrogel nanoparticle entity appreciably. Accordingly, the amount of the d-TPE molecule doped could dictate the detection sensitivity. In principal, single CrO_4^{2-} detection might become possible when one d-TPE molecule is doped to one hydrogel nanoparticle. The present design and synthesis offer a unified conceptual methodology to engineer functional nanomaterials that are sensitive to external stimuli, with the potential to advance the various applications.

ASSOCIATED CONTENT

Supporting Information

NMR of the d-TPE molecule (Figures S1 and S2); PL excitation and emission spectra of d-TPE solution and dP1 dispersion (Figure S3); SEM image of the dP2 core and GPC data of dP2 (Figure S4); Size parameters of dP1, dP2, and dP3 (Table S1); DLS analysis of the as-prepared nanoparticles (Figure S5); PL spectra of dP1, dP2, and dP3 during heating and cooling cycles (Figure S6); digital photos of hydrogel nanoparticle dispersions at different temperatures (Figure S7); PL spectra of dP1 at four heating−cooling cycles (Figure S8); PL spectra of the d-TPE doped PS-*co*-PAA nanoparticles during heating and cooling and a SEM image (Figure S9); PL spectra of the dP1 during a heating

dx.doi.org/10.1021/am501106x | ACS Appl. Mater. Interfaces 2014, 6, 4650−4657

and cooling cycle at pH 3 and pH 11 (Figure S10); PL spectra of the dP1 dispersions in the presence of Na_2SO_4, Na_2CO_3, $NaNO_2$, and $NaHCO_3$ from 10 to 50 °C (Figure S11); and PL spectra of the dP1 in pure water and in the presence of Na_2CrO_4 of different concentrations from 10 to 50 °C (Figure S12). This material is available free of charge via the Internet at http://pubs.acs.org.

AUTHOR INFORMATION

Corresponding Authors

*K.Y.: e-mail, kui.yu@nrc.ca.

*Q.L.: e-mail, linquan@jlu.edu.cn.

Author Contributions

⊥Y.J. and X.Y. contributed equally to this work.

Notes

The authors declare no competing financial interest.

ACKNOWLEDGMENTS

We thank Prof. Jingzhi Sun and Prof. Benzhong Tang for providing us the immobilization-induced emission (IIE) molecule, a tetraphenylethene derivative 1,2-bis[4-(2-triethylammonioethoxy)phenyl]-1,2-diphenylethene dibromide (d-TPE) which is a water-soluble ammonium salt, used in the present study. We thank Dr. Stephen Lang for useful discussions. This research was financially supported by the National Nature Science Foundation of China (Grants 21174048, 21304090, and 51373061), the National Basic Research Program (Grant 2012CB933802), and Programme of Introducing Talents of Discipline to Universities (111 Project B06009).

REFERENCES

(1) Gota, C.; Okabe, K.; Funatsu, T.; Harada, Y.; Uchiyama, S. Hydrophilic Fluorescent Nanogel Thermometer for Intracellular Thermometry. *J. Am. Chem. Soc.* **2009**, *131*, 2766−2767.

(2) Brites, C. D. S.; Lima, P. P.; Silva, N. J. O.; Millán, A.; Amaral, V. S.; Palacio, F.; Carlos, L. D. A Luminescent Molecular Thermometer for Long-Term Absolute Temperature Measurements at the Nanoscale. *Adv. Mater.* **2010**, *22*, 4499−4504.

(3) Zhang, X. Y.; Zhang, X. Q.; Wang, S. Q.; Liu, M.Y.; Zhang, Y.; Tao, L.; Wei, Y. Facile Incorporation of Aggregation-Induced Emission Materials into Mesoporous Silica Nanoparticles for Intracellular Imaging and Cancer Therapy. *ACS Appl. Mater. Interfaces* **2013**, *5*, 1943−1947.

(4) Qin, W.; Ding, D.; Liu, J. Z.; Yuan, W. Z.; Hu, Y.; Liu, B.; Tang, B. Z. Biocompatible Nanoparticles with Aggregation-Induced Emission Characteristics as Far-Red/Near-Infrared Fluorescent Bioprobes for in Vitro and in Vivo Imaging Applications. *Adv. Funct. Mater.* **2012**, *22*, 771−779.

(5) Yu, Y.; Feng, C.; Hong, Y. N.; Liu, J. Z.; Chen, S. J.; Ng, K. M.; Luo, K. Q.; Tang, B. Z. Cytophilic Fluorescent Bioprobes for Long-Term Cell Tracking. *Adv. Mater.* **2011**, *23*, 3298−3302.

(6) Dai, Y. L.; Ma, P. A.; Cheng, Z. Y.; Kang, X. J.; Zhang, X.; Hou, Z. Y.; Li, C. X.; Yang, D. M.; Zhai, X. F.; Lin, J. Up-Conversion Cell Imaging and pH-Induced Thermally Controlled Drug Release from $NaYF_4$:Yb^{3+}/Er^{3+}@Hydrogel Core-Shell Hybrid Microspheres. *ACS Nano* **2012**, *6*, 3327−3338.

(7) Kaewsaneha, C.; Tangboriboonrat, P.; Polpanich, D.; Eissa, M.; Elaissari, A. Janus Colloidal Particles: Preparation, Properties, and Biomedical Applications. *ACS Appl. Mater. Interfaces* **2013**, *5*, 1857−1869.

(8) Chang, B. S.; Chen, D.; Wang, Y.; Chen, Y. Z.; Jiao, Y. F.; Sha, X. Y.; Yang, W .L. Bioresponsive Controlled Drug Release Based on Mesoporous Silica Nanoparticles Coated with Reductively Sheddable Polymer Shell. *Chem. Mater.* **2013**, *25*, 574−585.

(9) Chen, L. Y.; Ou, C. M.; Chen, W. Y.; Huang, C. C.; Chang, H. T. Synthesis of Photoluminescent Au ND-PNIPAM Hybrid Microgel for the Detection of Hg^{2+}. *ACS Appl. Mater. Interfaces* **2013**, *5*, 4383−4388.

(10) Yin, L. Y.; He, C. S.; Huang, C. S.; Zhu, W. P.; Wang, X.; Xu, Y. F.; Qian, X. H. A Dual pH and Temperature Responsive Polymeric Fluorescent Sensor and Its Imaging Application in Living Cells. *Chem. Commun.* **2012**, *48*, 4486−4488.

(11) Studer, D.; Palankar, R.; Bédard, M.; Winterhalter, M.; Springer, S. Retrieval of a Metabolite from Cells with Polyelectrolyte Microcapsules. *Small* **2010**, *6*, 2412−2419.

(12) Toal, S. J.; Jones, K. A.; Magde, D.; Trogler, W. C. Luminescent Silole Nanoparticles as Chemoselective Sensors for Cr(VI). *J. Am. Chem. Soc.* **2005**, *127*, 11661−11665.

(13) Li, Z.; Dong, Y. Q.; Lam, J. W. Y.; Sun, J. X.; Qin, A. J.; Häußler, M.; Dong, Y. P.; Sung, H. H. Y.; Williams, I. D.; Kwok, H. S.; Tang, B. Z. Functionalized Siloles: Versatile Synthesis, Aggregation-Induced Emission, and Sensory and Device Applications. *Adv. Funct. Mater.* **2009**, *19*, 905−917.

(14) Hong, Y. N.; Xiong, H.; Lam, J. W. Y.; Häußler, M.; Liu, J. Z.; Yu, Y.; Zhong, Y. C.; Sung, H. H. Y.; Williams, I. D.; Wong, K. S.; Tang, B. Z. Fluorescent Bioprobes: Structural Matching in the Docking Processes of Aggregation-Induced Emission Fluorogens on DNA Surfaces. *Chem.—Eur. J.* **2010**, *16*, 1232−1245.

(15) Hong, Y. N.; Lam, J. W. Y.; Tang, B. Z. Aggregation-Induced Emission. *Chem. Soc. Rev.* **2011**, *40*, 5361−5388.

(16) Hong, Y. N.; Lam, J. W. Y.; Tang, B. Z. Aggregation-Induced Emission: Phenomenon, Mechanism and Applications. *Chem. Commun.* **2009**, 4332−4353.

(17) Shustova, N. B.; Ong, T. C.; Cozzolino, A. F.; Michaelis, V. K.; Griffin, R. G.; Dincă, M. Phenyl Ring Dynamics in a Tetraphenylethylene-Bridged Metal-Organic Framework: Implications for the Mechanism of Aggregation-Induced Emission. *J. Am. Chem. Soc.* **2012**, *134*, 15061−15070.

(18) Shustova, N. B.; McCarthy, B. D.; Dincă, M. Turn-On Fluorescence in Tetraphenylethylene-Based Metal-Organic Frameworks: An Alternative to Aggregation-Induced Emission. *J. Am. Chem. Soc.* **2011**, *133*, 20126−20129.

(19) Shi, J. Q.; Chang, N.; Li, C. H.; Mei, J.; Deng, C. M.; Luo, X. L.; Liu, Z. P.; Bo, Z. S.; Dong, Y. Q.; Tang, B. Z. Locking the Phenyl Rings of Tetraphenylethene Step by Step: Understanding the Mechanism of Aggregation-Induced Emission. *Chem. Commun.* **2012**, *48*, 10675−10677.

(20) Wang, J.; Mei, J.; Hu, R. R.; Sun, J. Z.; Qin, A. J.; Tang, B. Z. Click Synthesis, Aggregation-Induced Emission, *E*/*Z* Isomerization, Self-Organization, and Multiple Chromisms of Pure Stereoisomers of a Tetraphenylethene-Cored Luminogen. *J. Am. Chem. Soc.* **2012**, *134*, 9956−9966.

(21) Tang, L.; Jin, J. K.; Qin, A. J.; Yuan, W. Z.; Mao, Y.; Mei, J.; Sun, J. Z.; Tang, B. Z. A Fluorescent Thermometer Operating in Aggregation-Induced Emission Mechanism: Probing Thermal Transitions of PNIPAM in Water. *Chem. Commun.* **2009**, 4974−4976.

(22) Lai, C. T.; Chien, R. H.; Kuo, S.W.; Hong, J. L. Tetraphenylthiophene-Functionalized Poly(*N*-isopropylacrylamide): Probing LCST with Aggregation-Induced Emission. *Macromolecules* **2011**, *44*, 6546−6556.

(23) Yang, C. M.; Lai, Y. W.; Kuo, S. W.; Hong, J. L. Complexation of Fluorescent Tetraphenylthiophene-Derived Ammonium Chloride to Poly(*N*-isopropylacrylamide) with Sulfonate Terminal: Aggregation-Induced Emission, Critical Micelle Concentration, and Lower Critical Solution Temperature. *Langmuir* **2012**, *28*, 15725−15735.

(24) Yuan, W. Z.; Lu, P.; Chen, S. M.; Lam, J. W. Y.; Wang, Z. M.; Liu, Y.; Kwok, H. S.; Ma, Y. G.; Tang, B. Z. Changing the Behavior of Chromophores from Aggregation-Caused Quenching to Aggregation-Induced Emission: Development of Highly Efficient Light Emitters in the Solid State. *Adv. Mater.* **2010**, *22*, 2159−2163.

(25) Chung, J. W.; An, B. K.; Park, S. Y. A Thermoreversible and Proton-Induced Gel-Sol Phase Transition with Remarkable Fluorescence Variation. *Chem. Mater.* **2008**, *20*, 6750−6755.

(26) Luo, Z. T.; Yuan, X.; Yu, Y.; Zhang, Q. B.; Leong, D. T.; Lee, J. Y.; Xie, J. P. From Aggregation-Induced Emission of Au(I)-Thiolate Complexes to Ultrabright Au(0)@Au(I)-Thiolate Core-Shell Nanoclusters. *J. Am. Chem. Soc.* **2012**, *134*, 16662−16670.
(27) Qi, X. Y.; Li, H.; Lam, J. W. Y.; Yuan, X. T.; Wei, J.; Tang, B. Z; Zhang, H. Graphene Oxide as a Novel Nanoplatform for Enhancement of Aggregation-Induced Emission of Silole Fluorophores. *Adv. Mater.* **2012**, *24*, 4191−4195.
(28) Yuan, W. Z.; Gong, Y.Y.; Chen, S.M.; Shen, X. Y.; Lam, J. W. Y.; Lu, P.; Lu, Y.W.; Wang, Z.M.; Hu, R.R.; Xie, N.; Kwok, H. S.; Zhang, Y.M.; Sun, J.Z.; Tang, B. Z. Efficient Solid Emitters with Aggregation-Induced Emission and Intramolecular Charge Transfer Characteristics: Molecular Design, Synthesis, Photophysical Behaviors, and OLED Application. *Chem. Mater.* **2012**, *24*, 1518−1528.
(29) Chen, J. W.; Peng, H.; Law, C. C. W.; Dong, Y. P.; Lam, J. W. Y.; Williams, I. D.; Tang, B. Z. Hyperbranched Poly(phenylenesilolene)s: Synthesis, Thermal Stability, Electronic Conjugation, Optical Power Limiting, and Cooling-Enhanced Light Emission. *Macromolecules* **2003**, *36*, 4319−4327.
(30) Li, J.; Hong, X.; Liu, Y.; Li, D.; Wang, Y. W.; Li, J. H.; Bai, Y. B.; Li, T. J. Highly Photoluminescent CdTe/Poly(*N*-isopropylacrylamide) Temperature-Sensitive Gels. *Adv. Mater.* **2005**, *17*, 163−166.
(31) Jiang, Y. N.; Yang, X. D.; Ma, C.; Wang, C. X.; Li, H.; Dong, F. X.; Zhai, X. M.; Yu, K.; Lin, Q.; Yang, B. Photoluminescent Smart Hydrogels with Reversible and Linear Thermoresponses. *Small* **2010**, *6*, 2673−2677.
(32) Ballauff, M.; Lu, Y. "Smart" Nanoparticles: Preparation, Characterization and Applications. *Polymer* **2007**, *48*, 1815−1823.
(33) Tsuji, S.; Kawaguchi, H. Temperature-Sensitive Hairy Particles Prepared by Living Radical Graft Polymerization. *Langmuir* **2004**, *20*, 2449−2455.
(34) Xiao, D.; Wang, K. M.; Xiao, W. X. Synchronous Fluorescence and Absorbance Dynamic Liquid Drop Sensor for Cr(VI) Determination at the Femtomole Level. *Analyst* **2001**, *126*, 1387−1392.
(35) Ivask, A.; Virta, M.; Kahru, A. Construction and Use of Specific Luminescent Recombinant Bacterial Sensors for the Assessment of Bioavailable Fraction of Cadmium, Zinc, Mercury and Chromium in the Soil. *Soil Biol. Biochem.* **2002**, *34*, 1439−1447.
(36) Yang, X. D.; Jiang, Y. N.; Shen, B. W.; Chen, Y.; Dong, F. X.; Yu, K.; Yang, B.; Lin, Q. Thermo-Responsive Photoluminescent Polymer Brushes Device as a Platform for Selective Detection of Cr(VI). *Polym. Chem.* **2013**, *4*, 5591−5596.